5-1-2020

Analysis of the Inhibitory Potency, Oxime-mediated Reactivation Profile, and Binding Characteristics of Metabolites of Phorate

Luke Acuff
Mississippi State University

Analysis of the Inhibitory Potency, Oxime-mediated Reactivation Profile, and Binding Characteristics of Metabolites of Phorate.

By

William Luke Acuff

A Thesis
Submitted to the Faculty of
Mississippi State University
in Partial Fulfillment of the Requirements
for the *Cursus Honorum*

Mississippi State, Mississippi

April 9th, 2020

ACKNOWLEDGEMENTS

First, I would like to begin by expressing my most sincere gratitude for my research advisor and principle investigator, Dr. Janice Chambers. Her ever-present support, mentoring, and guidance have been critical to my success both at and beyond Mississippi State as I begin a career in research. She started my research path three years ago when I joined her lab, and since then, her countless and invaluable recommendations, critiques, and words of advice have substantially improved my skills as both an academic and as a person.

Additionally, I would like to thank Dr. Edward Meek for training me, offering guidance, and supervising me as I collected and compiled much of the data I am about to present. My success in pursuing this project would not be possible without his consistent and knowledgeable guidance. Of course, I would also like to thank the remainder of the Chambers lab for their patience, support, and collaboration over the past three years. I would like to again thank Dr. Meek and Shane Bennett for contributing data to this project. I would especially like to thank and acknowledge the late Dr. Howard Chambers, who designed the novel oximes that inspired much of this research.

Finally, I would like to thank and acknowledge:

Dr. Steven Gwaltney and Jerrano Bowleg for teaching me the ways of computational chemistry and for heavily contributing to the computational aspects of this project.

My family and community for supporting me as I performed this research.

The faculty and staff of Mississippi State University, the Bagley College of Engineering, and the Shackouls Honors College for educating me, preparing me for the future, and pushing me to write this thesis.

This research was funded by the National Institute of Health NIH R21 NS108954.

ABSTRACT

Organophosphates (OPs), used as insecticides and nerve agents, pose a severe threat to military personnel and civilians because of their potency as inhibitors of acetylcholinesterase (AChE). The OP insecticide phorate (rat oral LD50 1.4-3.7 mg/kg) is particularly toxic and could be used as a chemical weapon. Unlike similar OPs, phorate exhibits an unusual delay in the appearance of toxic signs in laboratory rats. Phorate has a more complex metabolism than most OPs: activation to phorate-oxon (PHO), then sulfoxidation to PHO-sulfoxide (PHX) and then to PHO-sulfone (PHS), which are increasingly more potent anticholinesterases. Additionally, PHO exhibits a different oxime-mediated reactivation profile than the well-studied OP paraoxon (PXN) which is also a diethyl phosphate. Two hypotheses, that PHO is bioactivated to its more potent metabolites PHX and PHS in the brain, and that PHO utilizes an unorthodox ethoxy leaving group, could help explain these differences between PHO and PXN. Analysis of OP scavenger carboxylesterase inhibition in rat liver by phorate metabolites indicates poor inhibition efficacy by PHX (IC 50: 420 nM) as compared to PHO and PHS (IC50: 20 or 32 nM, respectively); this could support the hypothesis of an alternative leaving group. Computational modeling (docking, molecular dynamics, quantum mechanics/molecular mechanics) is used to further determine the plausibility of the alternative leaving group hypothesis. Finally, oximes, like FDA-approved 2-PAM, can reactivate inhibited AChE, but 2-PAM is unable to penetrate the blood-brain barrier (BBB). MSU's novel substituted phenoxyalkyl pyridinium oximes (US patent 9,277,937) have been shown to reactivate inhibited AChE in the brain in animal tests. In vitro results showed levels of novel oxime AChE reactivation in rat brain preparations inhibited by PHO, PHX, or PHS that are comparable to those of 2-PAM. Initial in vivo results showed increased 24-hr survival compared to 2-PAM when novel oximes were administered following lethal doses of PHO in rats.

MSU’s novel oximes may lead to better protection from phorate poisoning. (Support: NIH R21 NS108954)

INTRODUCTION

Phorate, also known by the commercial name Thimet, is a highly neurotoxic chemical compound commonly used as a pesticide both within the US and abroad. Phorate is classified as an organophosphate (OP), a class of chemicals including other pesticides and nerve agents which operate by inhibiting the enzyme acetylcholinesterase (AChE) (US EPA, 2006). This inhibition leads to the buildup of the neurotransmitter acetylcholine (ACh) in synapses and neuromuscular junctions, which can cause permanent brain damage and death in humans (Moyer et al., 2018). Phorate itself is particularly toxic (rat oral LD50 1.4-3.7 mg/kg), and as such is classified as a restricted use pesticide in the United States, resulting in limited access for civilian use (US EPA, 2006). However, phorate remains abundant in developing nations and is accessible within the US, leading to concern that phorate's inconspicuous agricultural nature combined with its toxicity to humans make it a prime candidate for use as a chemical weapon by terrorists. This study is thus motivated to analyze phorate's properties as an anticholinesterase OP, as phorate is poorly studied in comparison to other OP pesticides and exhibits a variety of unorthodox behaviors. This behavior includes a delay in the onset of toxic signs in rat models following phorate exposure. Such a delay could be used as a terrorist strategy to induce panic in an exposed population. Additionally, phorate exhibits a different oxime mediated reactivation profile than the OP paraoxon (PXN), despite both OPs being diethyl phosphates. Finally, this study analyzes the effects of MSU's novel substituted phenoxyalkyl pyridinium oximes (US patent 9,277,937), on phorate metabolite-inhibited AChE, which may serve as a more effective therapy to combat phorate exposure due to the novel oximes' demonstrated ability to reactivate inhibited AChE in the brains of intact animals (Chambers et al., 2016; Dail et al., 2019).

Rather than directly producing inhibitory effects, phorate undergoes a specific metabolism in order to generate toxic metabolites (Fig. 1) (Moyer et al., 2018). The IC50 (concentration needed to inhibit 50% of AChE in a sample), of phorate is over 100,000 nM, indicating that phorate itself is not particularly inhibitory. Instead, phorate is bioactivated to a more toxic metabolite, phorate-oxon (PHO) (IC50 650 nM), by a class of enzymes known as cytochrome P450s (CYPs) (Chambers et al., 2018). PHO then may be further bioactivated by CYPs to phorate-oxon sulfoxide (PHX) (IC50 500 nM), and again to phorate-oxon sulfone (PHS) (IC50 350 nM). In comparison, the active metabolite of the pesticide parathion, PXN, has an IC50 of 23 nM. However, it is hypothesized that the more toxic metabolites PHX and PHS may be so reactive as to never escape the liver, which has very high CYP activity, indicating that PHO may be the only phorate metabolite actively circulating in the body (Nebert et al., 2013). Furthermore, CYPs in the brain may be capable of bioactivating PHO to PHX and PHS, potentially leading to formation of phorate's more toxic metabolites near critical target AChE in the central nervous system. The formation of more toxic metabolites in the brain following phorate exposure could help explain the observed delay in toxic signs following phorate exposure.

AChE, phorate's target, is an enzyme critical for neurological function in the body that is responsible for hydrolyzing the neurotransmitter ACh into its component parts: acetic acid and choline. During usual operation, ACh is hydrolyzed by interacting with AChE's catalytic triad located in the enzyme's active site. However, during inhibition by an OP such as PHO, the OP irreversibly binds to the serine group present in the catalytic triad, preventing ACh hydrolysis (Colović et al., 2013). This leads to the buildup of ACh in synapses and neuromuscular junctions, overstimulating them, which disrupts the function of the central and peripheral

nervous systems. That disruption promotes the onset of SLUD (salivation, lacrimation, urination, and defecation) symptoms and can lead to bradycardia, respiratory arrest, seizure, and death in humans (Peter et al., 2014).

Following exposure to OPs, either in pesticide or nerve agent form, treatment usually consists of a combination of atropine and an oxime reactivator. The drug atropine is an anticholinergic muscarinic antagonist, reducing effects of overstimulation by reducing ACh receptor activity. Oxime reactivators, however, are nucleophilic drugs intended to restore AChE function by removing the inhibiting phosphoryl group from the OP-bonded serine. Currently, the FDA approved oxime reactivator used for therapy following OP exposure is 2-PAM. However, 2-PAM has been shown to be ineffective at penetrating the blood-brain barrier (BBB), a highly selective semipermeable membrane that prevents some typically polar solutes from entering the extracellular fluid of the central nervous system (Abbott 2002; Chambers et al., 2016). This is problematic for the current class of approved oximes, pyridinium oximes, as they carry a permanent positive charge due to quaternary nitrogen in the pyridine ring. This is additionally problematic for OP exposure treatment as OPs like PXN and PHO permeate the BBB, and without oximes present, they can continue to wreak havoc on the central nervous system even after the current oximes are introduced as treatment. However, MSU has developed novel phenoxyalkyl pyridinium oximes (U.S. patent 9,277,937) that have demonstrated ability to cross the blood-brain barrier and attenuate brain damage in rats (Fig 3.) (Dail et al., 2019). As PHO is hypothesized to be bioactivated to its more toxic metabolites PHX and PHS in the brain, these novel oximes' ability to penetrate the BBB are even more critical when considering treatment for phorate exposure.

The exact interaction phorate's metabolites have with AChE is currently unknown, but it is hypothesized to be similar to PXN, a well-studied OP that operates by the traditional OP mechanism of phosphorylating the active site serine with release of the group designated as the "leaving group". During the interaction, PXN undergoes a substitution reaction in which the bond binding the central phosphate to its leaving group breaks, resulting in PXN's diethyl phosphate remaining irreversibly bound to the active site, inhibiting the enzyme (Kousba et al., 2004). PXN and PHO are both diethyl phosphates (Fig. 2), and as such, PHO is expected to follow a similar mechanism, binding to the active site serine while its sulfur-containing group behaves as the leaving group, resulting in a similar diethyl phosphate group remaining bound to the active site serine. However, PHO and PXN have exhibited different oxime reactivation profiles. As oxime mediated reactivation efficacy should primarily be influenced by what remains bound to the active site, PHO and PXN would be expected to exhibit similar reactivation profiles if they utilized similar leaving groups. Therefore, PHO is hypothesized to utilize an alternative leaving group, perhaps one of its ethoxy groups, during serine phosphorylation.

Exploring these hypotheses can be done in a variety of ways; however, for the purpose of this study, phorate's properties will be explored by analysis of its metabolites' inhibitory profile, oxime mediated reactivation profile, and binding characteristics. A metabolite's inhibitory profile, or its efficacy in inhibiting certain enzymes, can be tested *in vitro* by calculation of its IC50s. Butyrylcholinesterase (BChE) and carboxylesterase (CbxE) are also serine esterases and act as OP scavengers, or protective enzymes that can reduce OP toxicity by shielding more important enzymes like AChE by being inhibited by and thus inactivating incoming OPs (Masson and Lockridge, 2009; Hatfield et al., 2016). Comparing the differences between AChE,

BChE, and CbxE sensitivity to metabolites of phorate can offer clues to phorate's more complex metabolic pathway and binding profile.

Additionally, a metabolite's binding profile can be explored directly by computational simulation. By utilizing computational methods such as molecular docking, molecular dynamics, and quantum mechanics, PDB (Protein Data Bank) files representing the metabolite and its target enzyme can be manipulated and analyzed to compute approximate binding locations in addition to barrier heights, or energetic costs, of a given chemical reaction pathway (Case et al., 2018; Morris et al., 2009). In this way, the feasibility of phorate metabolites utilizing an alternative leaving group during AChE phosphorylation can be determined.

Finally, phorate's oxime-mediated reactivation profile can be examined by analyzing inhibited AChE reactivation efficacy assayed with various inhibitors (PXN, PHO, PHX, or PHS) and reactivators (2-PAM or selections from MSU's library of novel oximes). This difference can be quantified *in vitro* by biochemical reactivation assay or by *in vivo* survivability study. In either case, determining which oximes best protect against phorate will both bolster understanding of phorate's characteristics in addition to providing valuable information for how to best protect against potential phorate attacks in the future.

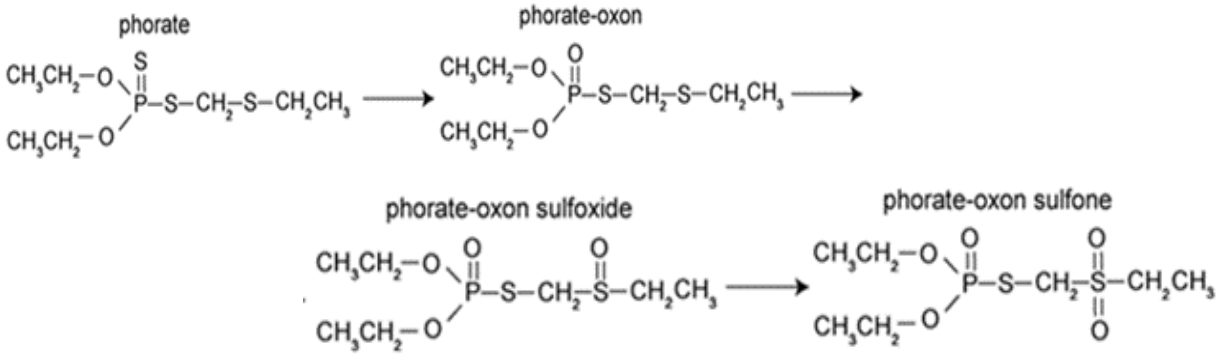

FIGURE 1: Phorate Metabolism

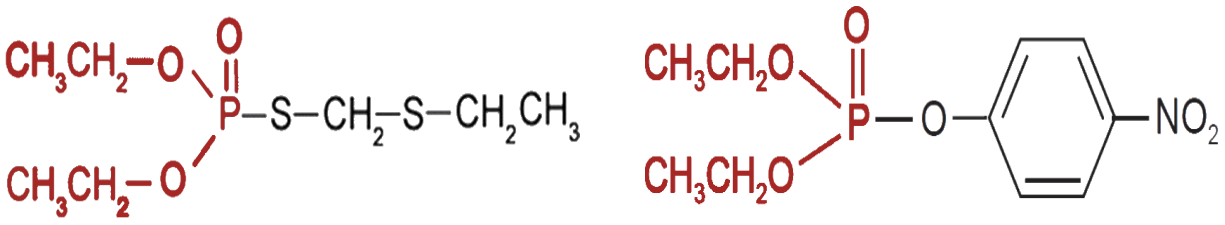

FIGURE 2: Phorate-Oxon (PHO, Left) and Paraoxon (PXN, Right) (Diethyl Phosphate Bolded)

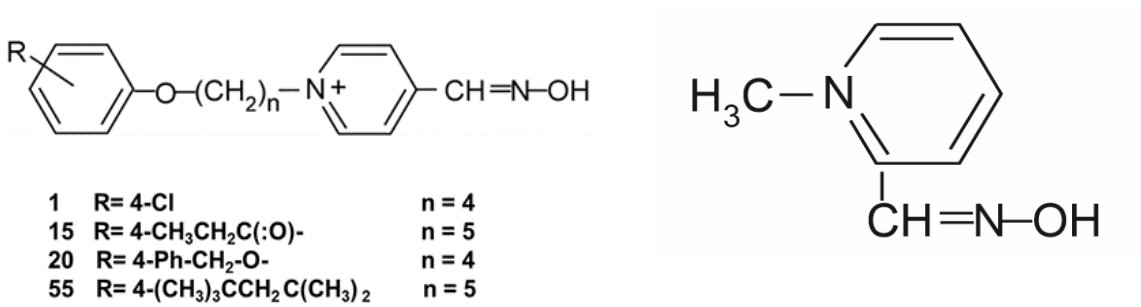

FIGURE 3: MSU's Novel Oxime Structures (Left, US patent 9,277,937) and 2-PAM Structure (Right)

METHODS

In vitro AChE, BChE, and CbxE Sensitivity

AChE, BChE, and CbxE sensitivity to phorate's toxic metabolites (PHO, PHX, and PHS) and PXN for comparison were assessed by calculation of the IC50 values for each respective metabolite and enzyme combination. To do this, a range of metabolite concentrations intended to induce 20% - 80% inhibition was established for each enzyme-metabolite combination (Table 1). Each combination's range was then assayed in a two-phase inhibition and analysis spectrophotometric assay. All concentrations are listed as final.

Inhibition Phase: For each metabolite-enzyme combination, 15 of 20 test tubes containing 2 mL of 10^{-4} mL/mL rat serum homogenate in 0.05 M Tris-HCl buffer (37°C, 7.4 pH) were incubated for 15 minutes at 37°C with various OP metabolite concentrations (Table 1). Two of the remaining tubes were similarly incubated with either 0.1 mM eserine-sulfate, a specific AChE and BChE inhibitor, or 0.01 mM PXN, a potent CbxE inhibitor, corresponding to the enzyme being assayed. The final three tubes were incubated with ethanol vehicle and served as uninhibited controls.

Analysis Phase: Each of the tubes was treated with either 1 mM acetylthiocholine substrate (AChE), 1 mM butyrylthiocholine substrate (BChE), or 0.5 mM nitrophenyl valerate (CbxE) and incubated for 15 minutes at 37°C. The reaction was then terminated by addition of 0.05% sodium dodecyl sulfate plus 5,5'-dithio-bis(nitrobenzoic acid) (DTNB; the chromogen) (AChE or BChE) or 0.02% sodium dodecyl sulfate (CbxE). The absorbance was quantified by a spectrophotometer at either 412 nm (AChE or BChE) or 405 nm (CbxE) (Ellman et al., 1961). Absorbance values for each metabolite-inhibited sample were corrected by subtraction of eserine sample absorbances, which served as blanks. They were then compared to uninhibited control

sample absorbances to generate percent inhibition. At least three replications were performed for metabolite-enzyme combination. IC50s were calculated for each combination by log-logit transformation of observed percent inhibitions.

	AChE	BChE	CbxE
PHO	5.62E-7 – 3.16E-6	3.16E-7 – 3.16E-6	1.00E-8 – 1.00E-7
PHX	1.78E-7 – 1.78E-6	1.00E-7 – 1.00E-6	1.78E-7 – 1.78E-6
PHS	5.62E-8 – 5.62E-7	3.16E-8 – 3.16E-7	1.78E-8 – 1.00E-7
PXN	5.62E-8 – 5.62E-7	5.62E-8 – 5.62E-7	5.62E-10 – 5.62E-9

TABLE 1: OP Concentration Ranges for AChE, BChE, and CbxE

In vitro AChE Reactivation Efficacy

In vitro AChE reactivation efficacy was assessed in rat brain homogenate by spectrophotometric assay divided into three phases: inhibition, reactivation, and analysis. Each assay featured 1 of 4 OP inhibitors (PXN, PHO, PHX, or PHS) and 5 oxime reactivators (2-PAM, and MSU 1, 15, 20 and 55). All concentrations are listed as final.

Inhibition Phase: For each assay, 5 of 6 1.5mL microcentrifuge tubes containing 1 mL of 1 mg/mL rat brain homogenate were incubated for 15 minutes at 37°C with one of the following OPs: $2.37 * 10^{-6}$ M PHO, 10^{-6} M PHX, 10^{-6} M PHS, or 10^{-7} M PXN. Concentrations were chosen to yield 80-90% inhibition compared to ethanol vehicle. The remaining tube was similarly incubated with ethanol vehicle to serve as an uninhibited control.

Reactivation Phase: Following inhibition, 100 μM of the following oximes were incubated for 30 minutes at 37°C, each in its own respective inhibited sample: MSU 1, 15, 20 or 55 or 2-PAM, or oxime vehicle (dimethyl sulfoxide: ethanol; 1:1).

Analysis Phase: Each tube was diluted (0.25 mL of sample into 9.75 mL 0.05 M Tris-HCl) and further portioned into 3 sub-samples (2 mL per sub-sample) and one 2 mL blank, which was treated with 0.1 mM eserine sulfate. After 15 minutes, each tube was treated with 1 mM acetylthiocholine substrate and incubated for an additional 15 minutes at 37°C. The reaction was then terminated by addition of 0.05% sodium dodecyl sulfate plus 5,5'-dithio-bis(nitrobenzoic acid) (DTNB; the chromogen). The absorbance was quantified in a spectrophotometer at 412 nm (Ellman et al., 1961; Chambers et al., 1988). Absorbance values for each sample were corrected by subtraction of eserine sample absorbances. Absorbance values were then compared to uninhibited control absorbances to generate percent inhibition. Percent inhibition values from reactivated samples were then compared to the percent inhibition of the unreactivated sample to generate percent reactivation. At least three replications were performed for each OP.

In Vivo 24-Hour Percent Survival in Rats Following Lethal Dose of PHO

An LD99 dosage (2.5 mg/kg; SC) of PHO (dissolved in Multisol) was established that was lethal within 24 hr to all rats treated with 0.65 mg/kg atropine (IM in saline). This dosage was also lethal within 24 hr to a moderate number of rats treated with atropine at 0.65 mg/kg (IM in saline) plus 2-PAM at 0.146 mmol/kg (human equivalent dosage for 3 autoinjectors; IM in Multisol). Oximes in Multisol were administered (IM) at 0.146 mmol/kg (2-PAM molar

equivalent dosage). Antidote (atropine +/- oxime) was administered at time of seizure onset (about 2 hours after PHO challenge). Rats were observed for the first 8 hours and 24-hour survival was recorded.

Computational Analysis (Docking, Molecular Dynamics)

To generate and prepare the AChE-OP complex for simulation, the X-ray crystal structure of the AChE (PDB code: 1F8U) was used. Partial atomic charges for PHO, PHX, and PHS were fitted with RESP charges adapted from the RED Server at the HF/6-31G*. (Bayly et al., 1993). Protonation states of all acidic and basic amino-acids residues were determined by the surrounding environment under physiological pH conditions (pH 7.4) using the H++ server (Gordon et at., 2005). Molecular docking calculations of the crystal structure were carried using the Autodock4.2 (AD4) software program through the graphical user interface AutoDockTools (ADT 1.5.4). The docking area was centered on the active site of the AChE and encompassed the residues of the catalytic triad. Hence, 100 separate docking calculations were performed using a Lamarckian Genetic Algorithm (Morris et al., 2009). This generated AChE-OP complexes for PHO, PHX, and PHS. Finally, the lowest energy binding pose provided by preliminary docking calculations was selected as the starting conformation for the subsequent molecular dynamics simulation. The ff14SB AMBER force field was used to assign bonded and nonbonded parameters to the protein. Hydrogen atoms were added to the PDB file via the LEAP module of the AMBER18. The system was solvated in an octahedron box of TIP3P water for a minimum distance of 10 Å on each side neutralized with sodium ions (Na+) (Maier et al., 2015; Jorgensen

et al., 1983; Åqvist, 1990). Ligand parameters were adapted from the GAFF force field using Antechamber (Wang et al., 2004; Wang et al., 2006).

MD simulations were then performed on each complex using the AMBER18 software package (Case et al., 2018). The simulation was performed under periodic boundary conditions and the long-range electrostatics were treated with the particle mesh Ewald method (Darden et al., 1993). The system temperature was maintained by the Langevin dynamics with a collision frequency of 1 ps^{-1} and the pressure was controlled by the Berendsen barostat with a pressure relaxation time of 1 ps (Uberuaga et al., 2004; Berendsen et al., 1984; Ryckaert et al., 1977). A cutoff distance of 12 Å was set for the nonbonded interactions and all covalent bonds that involve hydrogen atoms were constrained by the SHAKE algorithm, which allowed for a simulation timestep of 2 fs. Before the MD simulation, the system was energy minimized, first by energy minimizing the water molecules and counter ions and then by energy minimizing the whole system. After the initial minimization, the system was quickly heated up to 300 K in 100 ps using position restraints of 10.0 kcal mol^{-1} $Å^{-2}$ for the residues of the protein and the substrate. The system was further equilibrated using decreasing positional restraints, finishing equilibration without any restraints. During the optimization and equilibration steps, the distance between catalytic Ser199 hydroxyl oxygen and phosphorus atom of each substrate was restrained to 3.2 Å and all restraints were released for the production run. Subsequently, the whole system was simulated under an isothermal–isobaric (NPT) ensemble for 100 ns (300 K, 1 atm).

RESULTS

In vitro AChE, BChE, and CbxE Sensitivity

AChE and BChE followed the expected trend of PXN being the most potent inhibitor followed by PHS, then PHX, and finally PHO. In CbxE, PHO, PHS, and PXN were potent inhibitors; however, PHX was a comparatively poor inhibitor, with IC50 values 2 orders of magnitude greater than the other OPs.

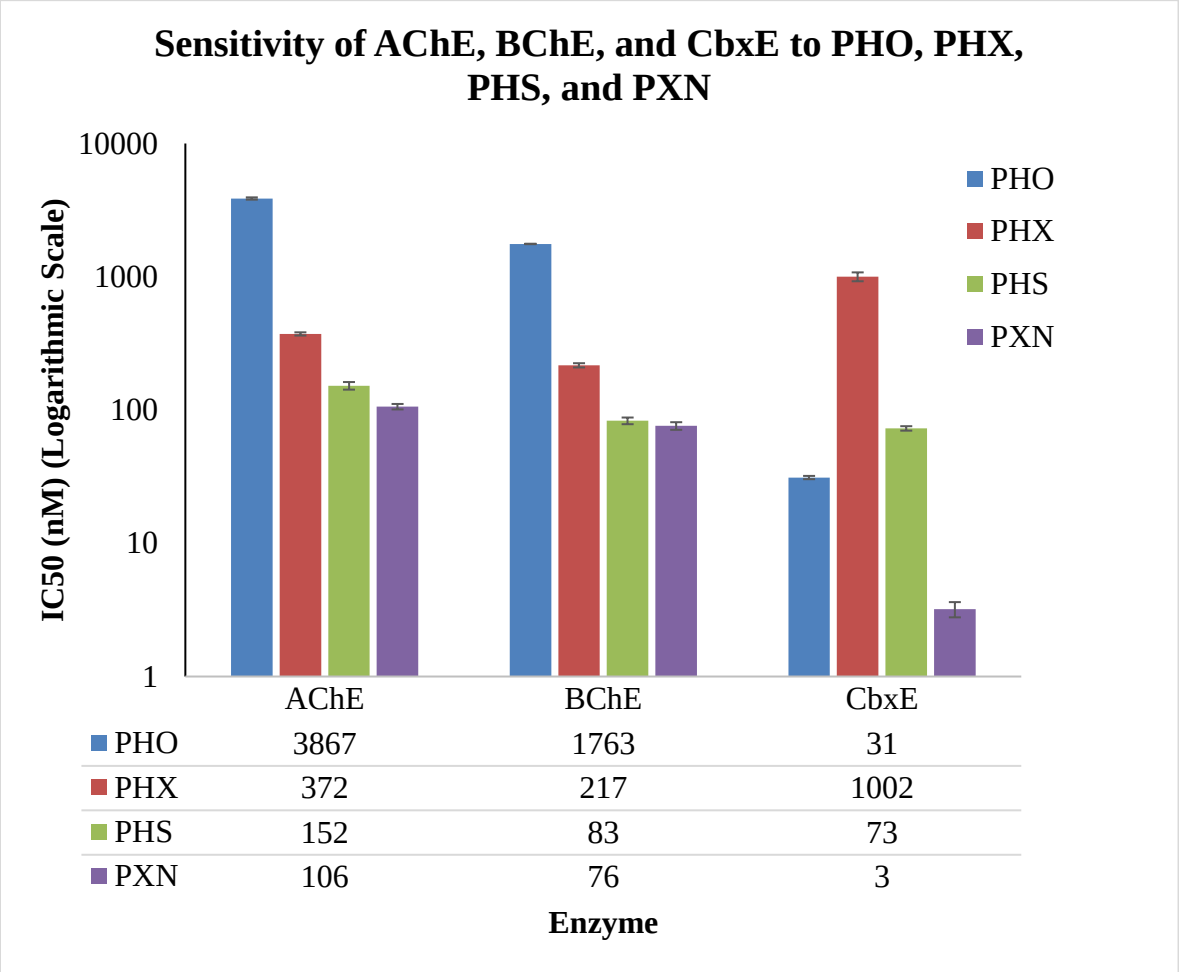

FIGURE 4: AChE, BChE, and CbxE IC50 (nM) of PHO, PHX, PHS, and PXN in Rat Serum (Logarithmic Scale) (Error Bars used Standard Error; number of replications = 3)

Computational Analysis (Docking, Molecular Dynamics)

Autodock4 generated 150 potential poses; the favorable poses were within the active site gorge of AChE. Further simulation using AMBER18 found that each OP was well positioned to interact with the catalytic triad of AChE (Serine 199, Histidine 433, and Glutamate 330).

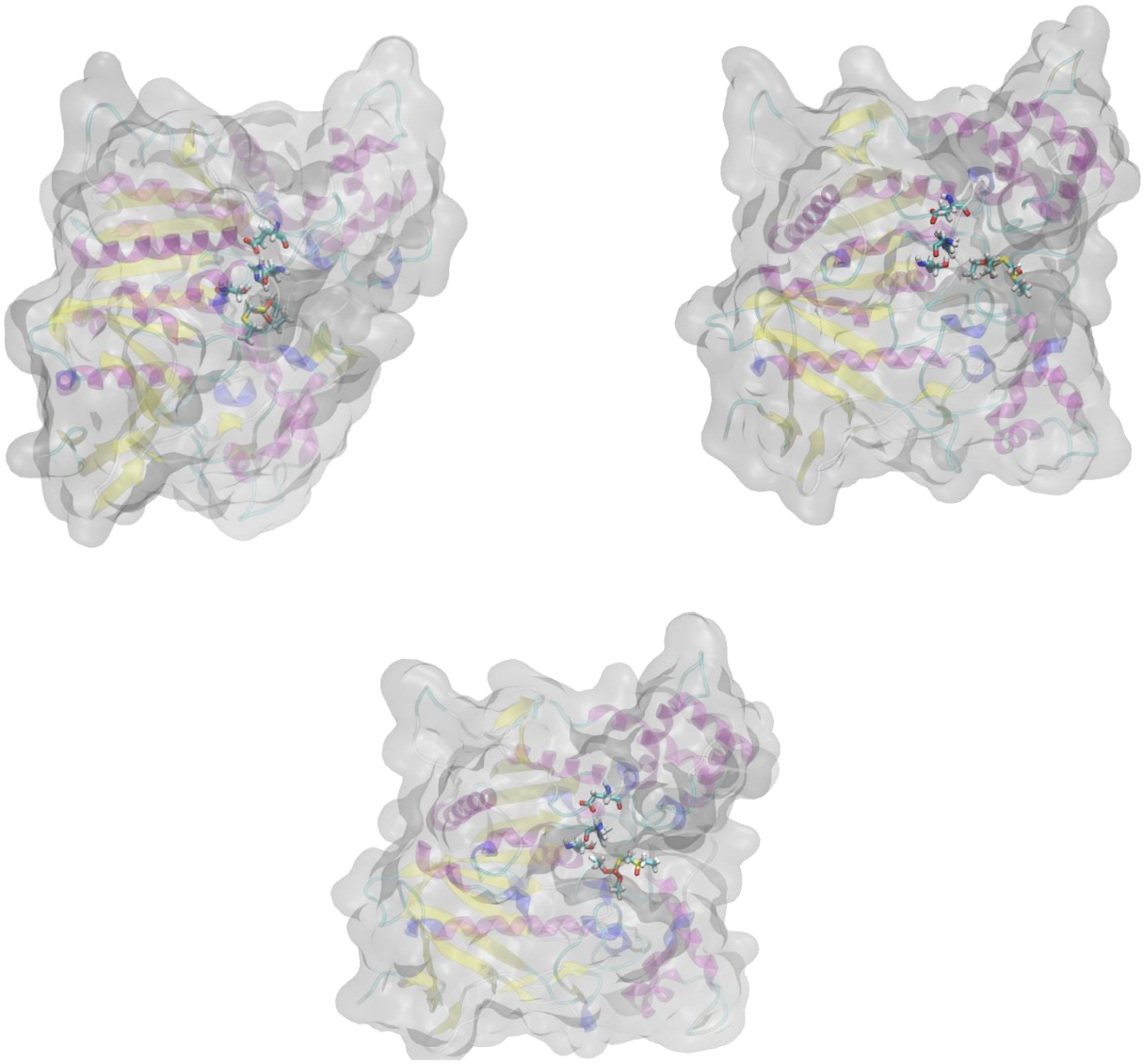

FIGURE 5: Binding of PHO, PHX, and PHS (Top Left, Top Right, Bottom Middle, respectively) to AChE (H: White, C: Cyan, O: Red, S: Yellow, N: Blue, P: Brown) (Images Generated using VMD (Humphrey et al., 1996))

In vitro AChE Reactivation Efficacy

Novel oximes MSU 1, 15, 20, and 55, and 2-PAM all provided some reactivation with PHO, PHX, and PHS. Overall, 2-PAM proved to be the most effective reactivator across all inhibitors except for PXN, which was most effectively reactivated by MSU 55.

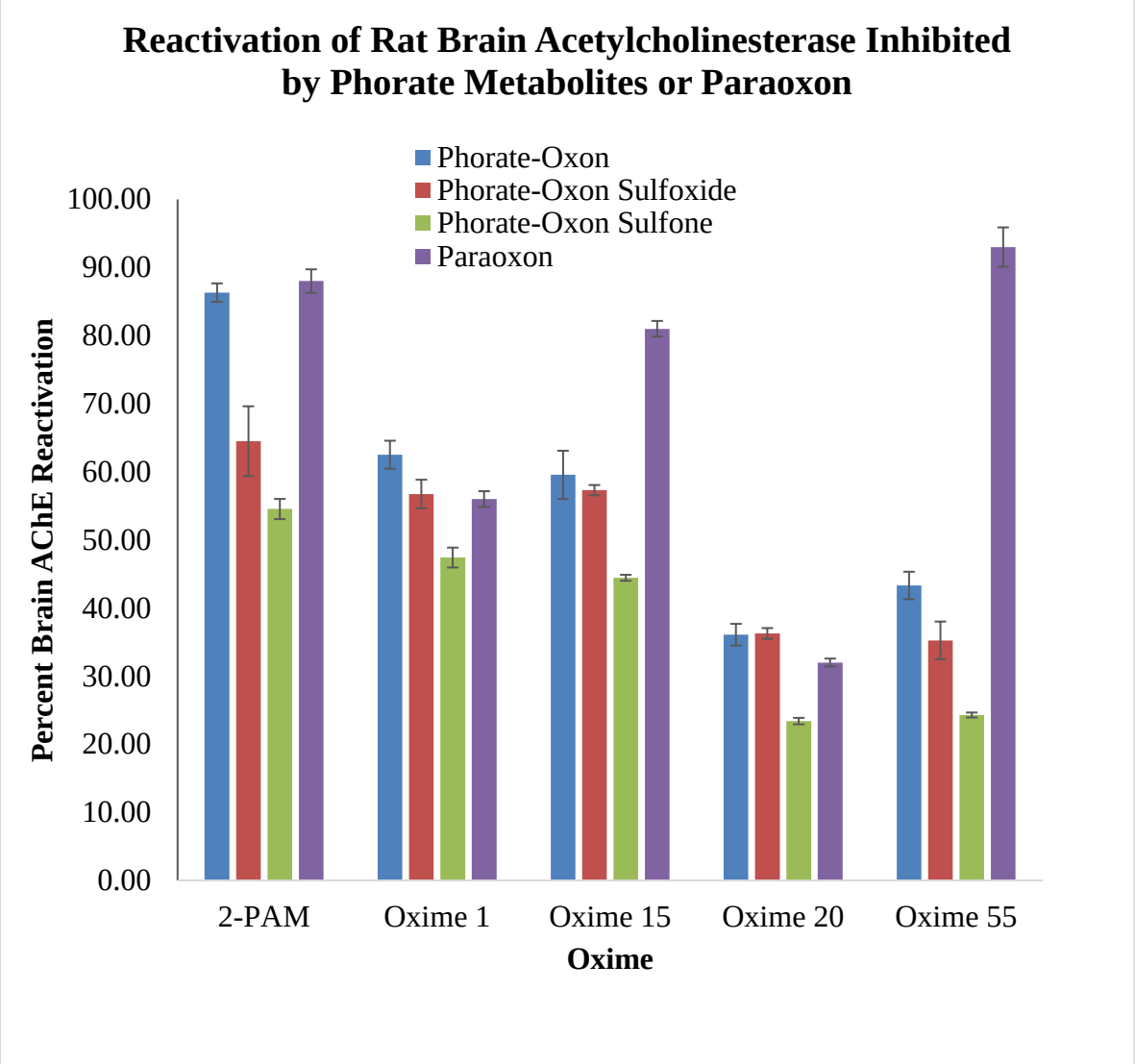

FIGURE 6: Percent reactivation following treatments of 2-PAM or MSU 1, 15, 20, or 55 (Error Bars used Standard Error; number of replications = 3)

In Vivo 24-Hour Percent Survival in Rats Following Lethal Dose of PHO

Following lethal doses of PHO, preliminary data show greater survivability in rats treated with MSU 15 and 55 over 2-PAM and MSU 20.

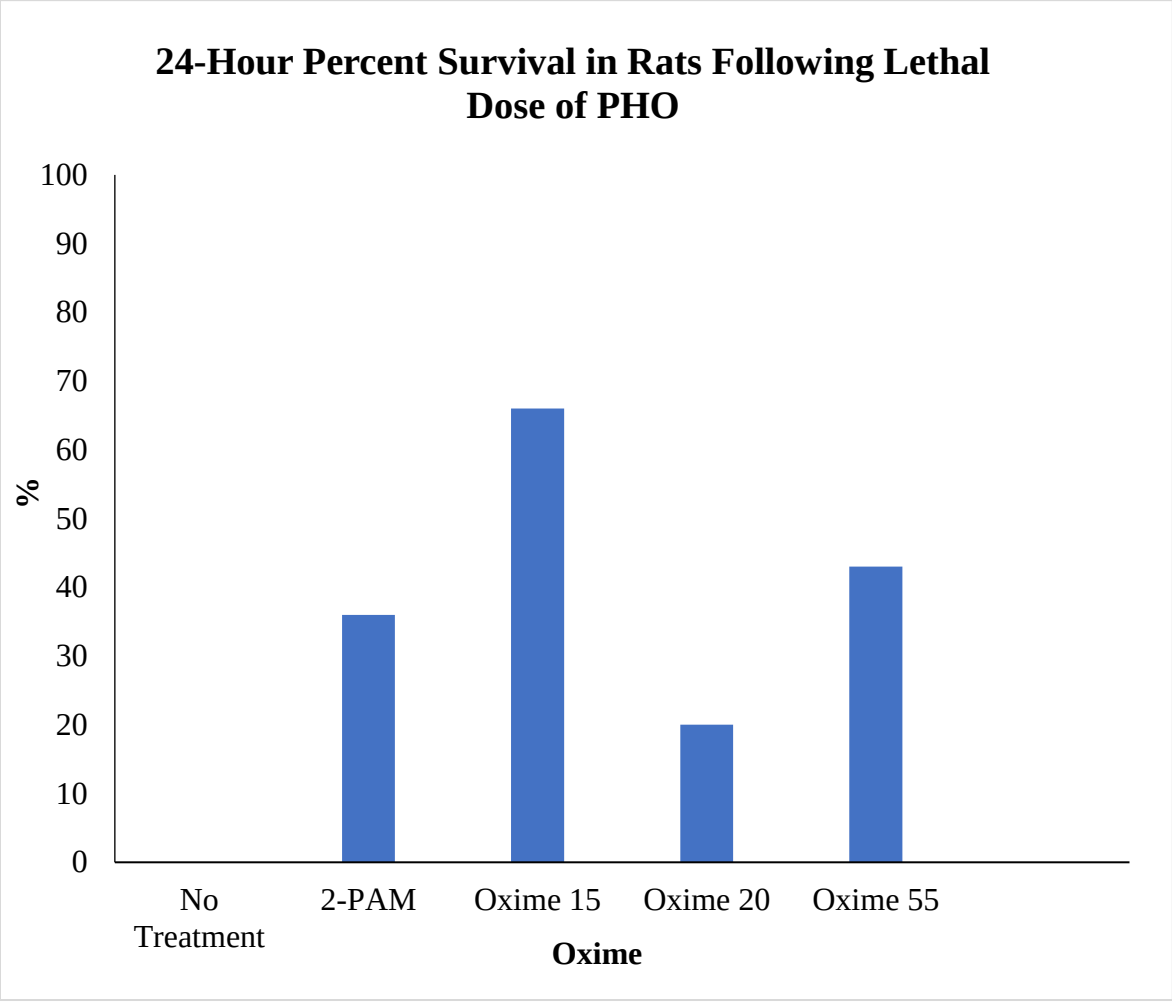

FIGURE 7: *In vivo* 24-Hour Percent Survival

DISCUSSION

In vitro AChE, BChE, and CbxE Sensitivity

Stoichiometric OP scavengers like BChE and CbxE protect AChE by covalently binding to OPs, preventing them from causing further inhibition. This study shows that metabolites of phorate are inhibitory to BChE and CbxE, and as such, we can expect those enzymes to produce protective effects. However, BChE and CbxE display surprisingly different inhibitory profiles in relation to the toxic metabolites of phorate. First, BChE exhibits a similar inhibition profile to AChE with PHO being inhibitory, PHX being more inhibitory, PHS being even more inhibitory, and PXN being the most inhibitory. As BChE and AChE are both cholinesterases, have very similar structures, and utilize similar – but not identical – active sites, it is no surprise that the two enzymes follow very similar inhibition trends (Chatonnet and Lockridge, 1989). However, CbxE exhibited a drastically different inhibitory profile, with PHX being weakly inhibitory compared to the other OPs, PHS being an order of magnitude more inhibitory than PHX, PHO – the parent compound of PHX and PHS – being even more inhibitory, and PXN being the most inhibitory, nearly 3 orders of magnitude more so than PHX. CbxE, while structurally similar to AChE and likely inhibited by the same process of covalent bonding to the active site serine, is not a cholinesterase, and as such is not expected to act in the exact same manner as AChE and BChE (Tsurkan et al., 2013). However, CbxE's failure to follow the general trend of phorate becoming more inhibitory as it is further bioactivated is a clear deviation from the norm.

This deviation could be the result of a variety of factors, including the previously hypothesized utilization of an alternative leaving group, as slight changes in active site chemistry (AChE vs CbxE) could cause different metabolites (PHO vs PHX) to utilize different leaving groups during inhibition. This is not guaranteed, however, as the sulfoxide group distinguishing

PHX from PHO could drastically change the binding efficacy when interacting with CbxE's active site as opposed to AChE. In either case, metabolites of phorate interact with CbxE in a way that is inherently different than with AChE and BChE.

Furthermore, CbxE's unorthodox inhibitory profile could alter its efficacy as a phorate metabolite scavenger and thus phorate's general metabolism. In particular, PHXs failure to effectively inhibit CbxE as compared to similar OPs could indicate that PHX does not interact as readily with CbxE, limiting its potential as a PHX stoichiometric scavenger. However, as CbxE is 50% inhibited by PHO at a concentration 2 orders of magnitude lower than AChE and BChE, distribution of phorate metabolites may only readily occur in regions of the body lacking high levels of protective CbxE. In humans, CbxE is readily expressed in the liver but is largely absent in the blood and brain (Hatfield et al., 2016). This disparity could limit phorate's inhibitory activity until phorate or PHO reaches the brain, contributing to both the observed delay in toxic signs and the hypothesized bioactivation of phorate to its more toxic metabolites in the brain. Additionally, CbxE circulates in the blood in rat models, potentially amplifying the delay even further in this study's *in vivo* models (Hatfield et al., 2016).

Computational Analysis (Docking, Molecular Dynamics)

Computational modeling results indicate what was expected of the traditional OP inhibition pathway: that PHO, PHX, and PHS energetically favor the active site gorge of AChE, and that they naturally position themselves to interact with AChE's catalytic triad. More important; however, are the poses that have been generated thus far by docking and molecular dynamics, which will be used to begin quantum mechanical analysis in order to generate barrier heights for alternative leaving groups. While this crucial quantum mechanical works remains to

be done, these first steps provide necessary sanity checks as to phorate metabolites' action and pave the way for future progress in determining the energetic feasibility of the alternative leaving group hypothesis.

In vitro AChE Reactivation Efficacy

In reactivating AChE inhibited by phorate metabolites, 2-PAM consistently achieved the greatest level of reactivation *in vitro*. However, MSU's novel oximes achieved comparable levels of reactivation, indicating that they are also capable of restoring AChE function. Additionally, AChE inhibited by more potent inhibitors – inhibitors with lower IC50s – were more difficult to reactivate for all tested oximes than AChE inhibited by their less potent counterparts with the notable exception of PXN. First, this trend serves as more evidence of the differences between PXN and phorate metabolite reactivation profiles. Furthermore, it indicates that the sulfoxide and later sulfone group gained during CYP bioactivation distinguishing PHX and PHS from PHO not only make the bioactivated compounds more inhibitory, but they also make the resulting OP-enzyme complex less susceptible to oxime nucleophilic attack. This indicates that the presumed leaving sulfur-containing group for phorate metabolites may interact with the OP-enzyme complex after covalent bonding of the OP to the serine; this assumption arises from the chemical structure of that group being the only observable difference between PHO, PHX, and PHS reactivation. That, in turn, lends more credence to the hypothesis of metabolites of phorate utilizing an alternative leaving group, distinguishing them from similar OPs.

In Vivo 24-Hour Percent Survival in Rats Following Lethal Dose of PHO

It is important to note that the data collected on *in vivo* survivability in rats are preliminary, as further testing has not been attempted due to the difficulties of obtaining consistent repetitions resulting from the observed delay in the onset of toxic signs. However, the data that have been collected indicate that MSU's novel oximes, specifically MSU 15 and 20, promote greater survivability than FDA approved 2-PAM. As *in vitro* data indicated that 2-PAM was a more effective reactivator than MSU's novel oximes, a disparity exists between *in vitro* reactivation efficacy and survivability. As MSU's novel oximes have been shown to penetrate the BBB (Chambers et al., 2016), survivability is likely increased by reactivation of rat AChE located in the brain. Protecting the brain is a critical step in combating any OP poisoning; however, as phorate is hypothesized to be bioactivated to its more toxic metabolites in the brain, the capability of oximes to penetrate the brain is perhaps even more important when combating phorate poisoning.

CONCLUSION

This study was designed to analyze various properties of phorate's metabolites in order to better understand the toxic pesticide's characteristics should it ever be used as a chemical weapon. While more analysis is needed to draw a clearer picture of those metabolites' binding action and metabolism, there are several conclusions that can be drawn from this study that help both explain phorate's unorthodox behavior and provide clues as to how to best combat it.

First, BChE and CbxE were shown to be inhibited by various concentrations of PHO, PHX, and PHS, indicating that these traditional stoichiometric OP scavengers play a part in protecting AChE during phorate exposure. This understanding will assist in the interpretation of phorate metabolite inhibition of AChE among different tissue samples with various concentrations of protective enzyme, in addition to predicting differences between human and rat models.

Furthermore, as indicated by computational modeling, phorate's metabolites likely follow the traditional pathway of binding to the active site serine during AChE inhibition. However, given the variety of inhibition and reactivation profiles exhibited by PHO, PHX, PHS, and PXN, the 'assumed leaving group' clearly plays a large role in characterizing the behavior of each individual metabolite, whether it is confirmed to be the true leaving group or not.

As for combating phorate poisoning, MSU's novel oximes have been shown to be effective, if not more effective, than 2-PAM, at reactivating phorate metabolite-inhibited rat brain AChE *in vitro*. Additionally, preliminary *in vivo* data support the efficacy and importance of BBB penetrating novel oximes when combating phorate poisoning.

While this study does not provide evidence that strongly supports the two proposed hypotheses – that phorate is bioactivated to its more toxic metabolites in the brain and that PHO

utilizes an alternative leaving group – it does provide data that are consistent with both hypotheses and could lead to further support if more analyses, specifically quantum mechanical and *in vivo*, are completed.

Ultimately, this study demonstrates the complexity of phorate's biochemistry and the need for better understanding of its variety of profiles and behaviors. Finally, it emphasizes the potential value of brain penetrating oximes when combating phorate poisoning, as protection of the brain remains a crucial aspect of combating OP exposure, potentially even more so with regard to phorate.

REFERENCES

Abbott NJ. 2002. Astrocyte–endothelial interactions and blood–brain barrier permeability. *J. Anat.* (2002) 200, pp629–638

Bayly CI, Cieplak P, Cornell W, Kollman PA. 1993. A well-behaved electrostatic potential based method using charge restraints for deriving atomic charges: the RESP model, *J. Phys. Chem*., 1993, 97, 10269-10280

Berendsen HJC, Postma JPM, Van Gunsteren WF, Dinola A, Haak JR. 1984. Molecular Dynamics with Coupling to An External Bath. *J. Chem. Phys.* 1984, 81, 3684– 3690, DOI: 10.1063/1.448118

Case DA, Ben-Shalom IY, Brozell SR, Cerutti DS, Cheatham TE, Cruzeiro WD, Darden TA, Duke RA, Ghoreishi D, Gilson MK, Gohlke H, Goetz AW, Greene D, Harris R, Homeyer N, Izadi S, Kovalenko A, Kurtzman T, Lee TS, LeGrand S, Li P, Lin C, Liu J, Luchko T, Luo R, Mermelstein DJ, Merz KM, Miao Y, Monard G, Nguyen C, Nguyen H, Omelyan I, Onufriev A, Pan F, Qi R, Roe DR, Roitberg A, Sagui C, Schott-Verdugo S, Shen J, Simmerling CL, Smith J, Salomon-Ferrer R, Swails J, Walker RC, Wang J, Wei H, Wolf RM, Wu X, Xiao L, York DM, Kollman PA. 2018. AMBER 2018, University of California, San Francisco.

Chambers JE. Gwaltney SR, Ross M. 2018. Identification of novel brain-penetrating oxime antidotes for phorate toxicity. NIH Exploratory/Developmental Grant, 1R21NS108954-01

Chambers JE, Meek EC, Bennett JP, Bennett WS, Chambers HW, Leach CA, Pringle RB, and Willis RW. 2016. Novel substituted phenoxyalkyl pyridinium oximes enhance survival and attenuate seizure-like behavior of rats receiving lethal levels of nerve agent surrogates. *Toxicology* 339:51-57.

Chambers JE, Wiygul SM, Harkness JE, Chambers HW. Effects of acute paraoxon and atropine exposures on retention of shuttle avoidance behavior in rats. 1988. *Neurosci. Res. Commun.* 3, 85–92.

Chatonnet A and Lockridge O. 1989. Review Article: Comparison of butyrylcholinesterase and acetylcholinesterase. *Biochem J*. 260, 625-634

Colović MB, Krstić DZ, Lazarević-Pašti TD, Bondžić AM, Vasić VM. 2013. Acetylcholinesterase inhibitors: pharmacology and toxicology. *Curr Neuropharmacol*. 2013;11(3):315–335. doi:10.2174/1570159X11311030006

Dail MB, Leach CA, Meek EC, Olivier AK, Pringle RB, Green CE, Chambers JE. 2019. Novel Brain-Penetrating Oxime Acetylcholinesterase Reactivators Attenuate Organophosphate-Induced

Neuropathology in the Rat Hippocampus. *Toxicol Sci.* 169(2):465-474. doi: 10.1093/toxsci/kfz060.

Darden T, York D, Pedersen L. 1993. Particle Mesh Ewald: An N·log(N) Method for Ewald Sums in Large Systems. *J. Chem. Phys.* 1993, 98, 10089– 10092, DOI: 10.1063/1.464397

Ellman GL, Courtney KD, Andrew V, Feather-stone RM. 1961. A new and rapid colorimetric determination of acetylcholinesterase activity. *Biochem Pharmacol*. 10.1016/0006-2952(61)90145-9

Gordon JC, Myers JB, Folta T, Shoja V, Heath LS, Onufriev A. 2005. H++: A Server for Estimating pKas and Adding Missing Hydrogens to Macromolecules. *Nucleic Acids Res.* 2005, *33*, W368– W371, DOI: 10.1093/nar/gki464

Hatfield MJ, Umans RA, Hyatt JL, et al. 2016. Carboxylesterases: General detoxifying enzymes. *Chem Biol Interact*. 2016;259(Pt B):327–331. doi:10.1016/j.cbi.2016.02.011

Humphrey W, Dalke A. Schulten K. 1996. VMD - Visual Molecular Dynamics. *J. Molec. Graphics*. 1996. vol. 14, pp. 33-38.

Jorgensen WL, Chandrasekhar J, Madura JD, Impey RW, Klein ML. 1983. Comparison of Simple Potential Functions for Simulating Liquid Water. *J. Chem. Phys.* 1983, 79, 926– 935, DOI: 10.1063/1.445869

Kousba AA, Sultatos LG, Poet TS, Timchalk C. 2004. Comparison of Chlorpyrifos-Oxon and Paraoxon Acetylcholinesterase Inhibition Dynamics: Potential Role of a Peripheral Binding Site. *Toxicol Sci.* 2004 Aug;80(2):239-48.

Maier JA, Martinez C, Kasavajhala K, Wickstrom L, Hauser KE, Simmerling C. 2015. ff14SB: Improving the Accuracy of Protein Side Chain and Backbone Parameters from ff99SB. *J. Chem. Theory Comput*. 2015, 11, 3696– 3713, DOI: 10.1021/acs.jctc.5b00255

Masson P and Lockridge O. 2009. Butyrylcholinesterase for protection from organophosphorus poisons: catalytic complexities and hysteretic behavior. *Arch Biochem Biophys*. 2010;494(2):107–120. doi:10.1016/j.abb.2009.12.005

Morris GM., Huey R, Lindstrom W, Sanner MF, Belew RK, Goodsell DS, Olson AJ. 2009. Autodock4 and AutoDockTools4: automated docking with selective receptor flexiblity. *J. Computational Chemistry* 2009, 16: 2785-91.

Moyer RA, McGarry KG Jr, Babin MC, Platoff GE Jr, Jett DA, Yeung DT. 2018. Kinetic analysis of oxime-assisted reactivation of human, Guinea pig, and rat acetylcholinesterase inhibited by the organophosphorus pesticide metabolite phorate oxon (PHO). *Pestic Biochem Physiol*. 2018;145:93–99. doi:10.1016/j.pestbp.2018.01.009

Nebert DW, Wikvall K, Miller WL. 2013. Human cytochromes P450 in health and disease. *Philos Trans R Soc Lond B Biol Sci*. 2013;368(1612):20120431. doi:10.1098/rstb.2012.0431

Peter JV, Sudarsan TI, Moran JL. 2014. Clinical features of organophosphate poisoning: A review of different classification systems and approaches. *Indian J Crit Care Med*. 2014;18(11):735–745. doi:10.4103/0972-5229.144017

Ryckaert JP, Ciccotti G, Berendsen HJC. 1977. Numerical Integration of the Cartesian Equations of Motion of a System with Constraints: Molecular Dynamics of n-Alkanes. *J. Comput. Phys.* 1977, 23, 327– 341, DOI: 10.1016/0021-9991(77)90098-5

Tsurkan LG, Hatfield MJ, Edwards CC, Hyatt JL, Potter PM. 2013. Inhibition of human carboxylesterases hCE1 and hiCE by cholinesterase inhibitors. *Chem Biol Interact*. 2013;203(1):226–230.doi:10.1016/j.cbi.2012.10.018

Uberuaga BP, Anghel M, Voter AF. 2004. Synchronization of Trajectories in Canonical Molecular-Dynamics Simulations: Observation, Explanation, and Exploitation. *J. Chem. Phys.* 2004, 120, 6363– 6374, DOI:10.1063/1.1667473

United States Environmental Protection Agency. 2006. Finalization of Interim Reregistration Eligibility Decisions (IREDs) and Interim Tolerance Reassessment and Risk Management Decisions (TREDs) for the Organophosphate Pesticides, and Completion of the Tolerance Reassessment and Reregistration Eligibility Process for the Organophosphate Pesticides. https://archive.epa.gov/pesticides/reregistration/web/pdf/phorate_ired.pdf

Wang J, Wolf RM, Caldwell JW, Kollman PA, Case DA. 2004. Development and Testing of a General Amber Force Field *J. Comput. Chem*. 2004, 25, 1157– 1174

Wang J, Wang W, Kollman PA, Case DA. 2006. Automatic Atom Type and Bond Type Perception in Molecular Mechanical Calculations *J. Mol. Graphics Modell*. 2006, 25, 247– 260

Åqvist, J. 1990. Ion-water Interaction Potentials Derived from Free Energy Perturbation simulations. *J. Phys. Chem*. 1990, 94, 8021– 8024, DOI: 10.1021/j100384a009